

# Recovery in Spider Silk Fibers

M. Elices, J. Pérez-Rigueiro, G. Plaza, G. V. Guinea

Departamento de Ciencia de Materiales, ETSI Caminos, Universidad Politécnica de Madrid, 28040 Madrid, Spain

Received 11 December 2003; accepted 23 January 2004

**ABSTRACT:** The extreme toughness of spider silk is dependent on the silk's ability to dissipate most of the mechanical energy imparted to the fiber during loading processes through irreversible deformations. This basic property makes the tensile behavior of spider silk fibers depend on the silk's previous deformation history in a largely unpredictable way. The resulting variability often represents an insurmountable difficulty for both the characterization of the material and its practical usage. In this study, it was

shown that spider silk is endowed with a property that allows to circumvent these problems: supercontraction, the large shrinkage of the longitudinal dimension of spider silk fibers in wet environments, recovers the tensile properties of deformed spider silk fibers in a repetitive and reproducible way. © 2004 Wiley Periodicals, Inc. *J Appl Polym Sci* 92: 3537–3541, 2004

**Key words:** biofibers; biopolymers; mechanical properties

## INTRODUCTION

There is considerable interest in the study of the relationship between the structure and mechanical properties of spider silks as a guide to the design and commercial production of protein-based fibers through genetic engineering.<sup>1,2</sup> However, spider silk has a number of inconveniences that may cast doubts on its practical usage, including a large variability in its mechanical properties, as revealed by tensile tests,<sup>3–5</sup> and the irreversible modification of its tensile behavior as a result of large deformations.<sup>6,7</sup> These are major hindrances both in the search for structure–property relations because most conclusions have been blurred by a large scatter in the tests<sup>3,5,8</sup> and in the implementation of spider silk as a structural material because irreversibility makes the behavior depend on the previous loading history.

It has been known for a long time that if an unrestrained spider silk fiber spun from the major ampullate gland (MAS) is submerged in water, it shortens substantially, a phenomenon known as supercontraction (SC),<sup>9</sup> and its stiffness drops by several orders of magnitude. Research by Gosline et al.<sup>10</sup> revealed that SC has profound implications on the mechanical behavior of spider silk, even suggesting a relationship between the microstructure and the tensile proper-

ties.<sup>11,12</sup> Exploring the behavior of spider silk fibers subjected to SC, we found that SC modifies the tensile properties of spider silk,<sup>13</sup> although the initial results were restricted to fibers obtained by forced silking and were, consequently, of limited practical use. In this study, we show that SC further allows the silk to overcome the aforementioned drawbacks independently from the origin or previous loading history of the fibers. This technique gives us a key to understanding some aspects of the fiber tensile behavior, such as the role of humidity and tensile stress in the viscoplastic response of spider silk fibers, and it should have far-reaching commercial implications.

## EXPERIMENTAL

Silk fibers from *Argiope trifasciata* spiders were used in this study. *A. trifasciata* is a common orb-web-building species of the Mediterranean coast that can be bred in captivity and whose size allows easy manipulation. Silk fibers were collected with two different procedures: naturally spun (NS) fibers were either retrieved from the spider web or from the safety line, and forcibly silked (FS) fibers were obtained by pulling the silk fiber from the spider at a controlled speed of 1 cm/s.<sup>14–16</sup>

The SC of silk was achieved as described elsewhere.<sup>13</sup> Briefly, samples were glued on perforated aluminum foil frames by their ends,<sup>17</sup> and we obtained SC by decreasing and fixing the gauge length at a value of  $L_0 - \Delta$ , where  $L_0$  is the initial gauge length and  $\Delta$  is the allowed reduction in the fiber's length. Samples were immersed in water for 30 min and allowed to dry overnight (nominal conditions: 20°C, relative humidity = 35%). Processes in which the fiber fully supercontracted the fixed  $\Delta$  value and the fiber remained stressed were labeled as controlled SC. For

Correspondence to: M. Elices (melices@mater.upm.es).

Contract grant sponsor: Ministerio de Ciencia y Tecnología (Spain); contract grant numbers: MAT 2000-1334 and MAT 2003-04906.

Contract grant sponsor: Comunidad de Madrid; contract grant number: 07N/0001/2002.

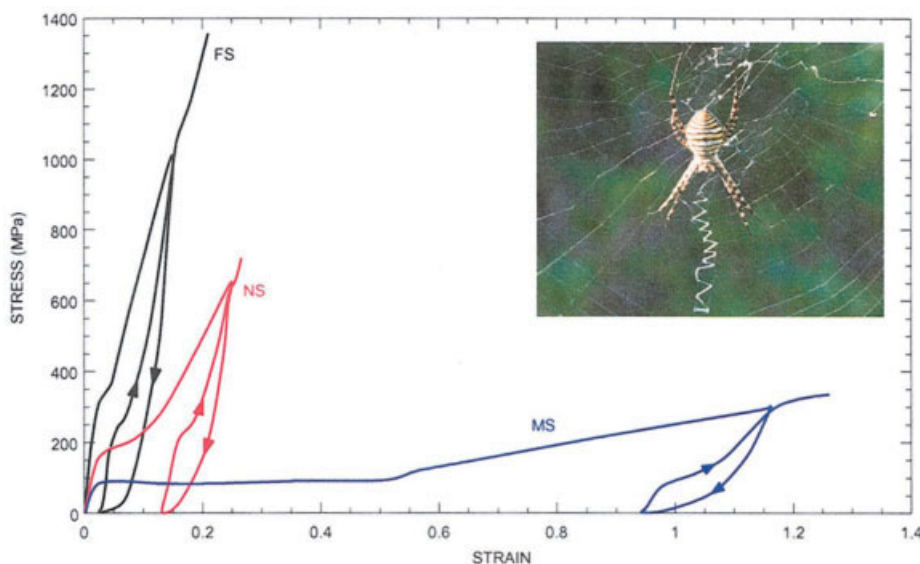


**Figure 1** Stress–strain curves of FS, NS, and MS spider silk (MAS from *A. trifasciata*; see inset). Also shown are the stress–strain curves after an unloading and reloading cycle.

high enough values of  $\Delta$ , SC did not reach the full  $\Delta$  value, and the fiber remained unstressed. These processes were labeled as maximum SC. The distance between the glued unstressed ends of the fiber after SC<sup>18</sup> ( $L_C$ ) was taken as the base length of the supercontracted samples. The SC process was labeled by the SC percentage, defined as  $(L_0 - L_C)/L_0$ .

Tensile tests were performed on an Instron 4411 testing machine (Canton, MA) at a constant crosshead speed to achieve an average strain rate of  $2 \times 10^{-4} \text{ s}^{-1}$ . The load applied to the sample was measured with a balance (AND 1200 G, resolution  $\pm 10 \text{ mg}$ ; Peabody, MA) attached to the lower end of the sample. The crosshead displacement was taken as a direct measurement of the sample deformation because the compliance of silk has been estimated as 1000 times larger than that of the equipment.<sup>19</sup> The tests were performed in air at 20°C and 35% relative humidity.

Some selected control and supercontracted samples were metallized before tensile testing and were observed in a scanning electron microscope (JEOL 6300, Tokyo, Japan) to measure the cross-sectional area. Force–displacement curves were scaled as stress–strain curves by the division of the force by the cross-sectional area (engineering stress) and the displacement by  $L_C$  (engineering strain).

## RESULTS AND DISCUSSION

Representative stress–strain curves of FS, NS, and maximal supercontracted (MS) fibers are shown in Figure 1, which illustrates both the variability of the stress–strain curves and the irreversible effect of large deformations. Here, two types of curves are depicted:

noval stress–strain curves and curves after an unloading and reloading cycle. The reloading behavior was completely different (particularly for NS and MS fibers) from the noval behavior. All of these curves came from the same spider and from the same type of silk, from the major ampullate gland.

First, we show that it was possible to gather the FS and NS stress–strain curves into a single reference curve by means of maximum SC. Figure 2(a) shows the stress–strain curves of noval FS and NS fibers before and after maximum SC. Both curves merged completely, although they were very different initially. Figure 2(b) shows the stress–strain curves of reloaded FS, NS, and MS fibers before and after recovery through maximum SC. Once more, all three recovered curves merged into the same reference curve, indistinguishable from the corresponding curve shown in Figure 2(a). In Figure 2(b), the stresses and strains were computed from the initial values of cross-section and fiber length at the points of reloading under the hypothesis that the volume of the fiber remained constant throughout the process.<sup>19</sup>

We show, then, that it was possible to obtain any NS stress–strain curve via controlled SC, starting from noval fibers or—and this is a major novelty—from reloaded (and, hence, irreversibly deformed) fibers. Figure 3(a) shows the stress–strain curves of noval FS and NS fibers before and after controlled SC. The purpose of this experiment was to obtain in a repetitive and reproducible way a stress–strain curve of the NS family.<sup>5</sup> The different initial curves (FS and NS) merged into the same curve. The same curve could be regained starting from reloaded fibers, as shown in Figure 3(b), in which reloaded FS, NS, and MS fibers

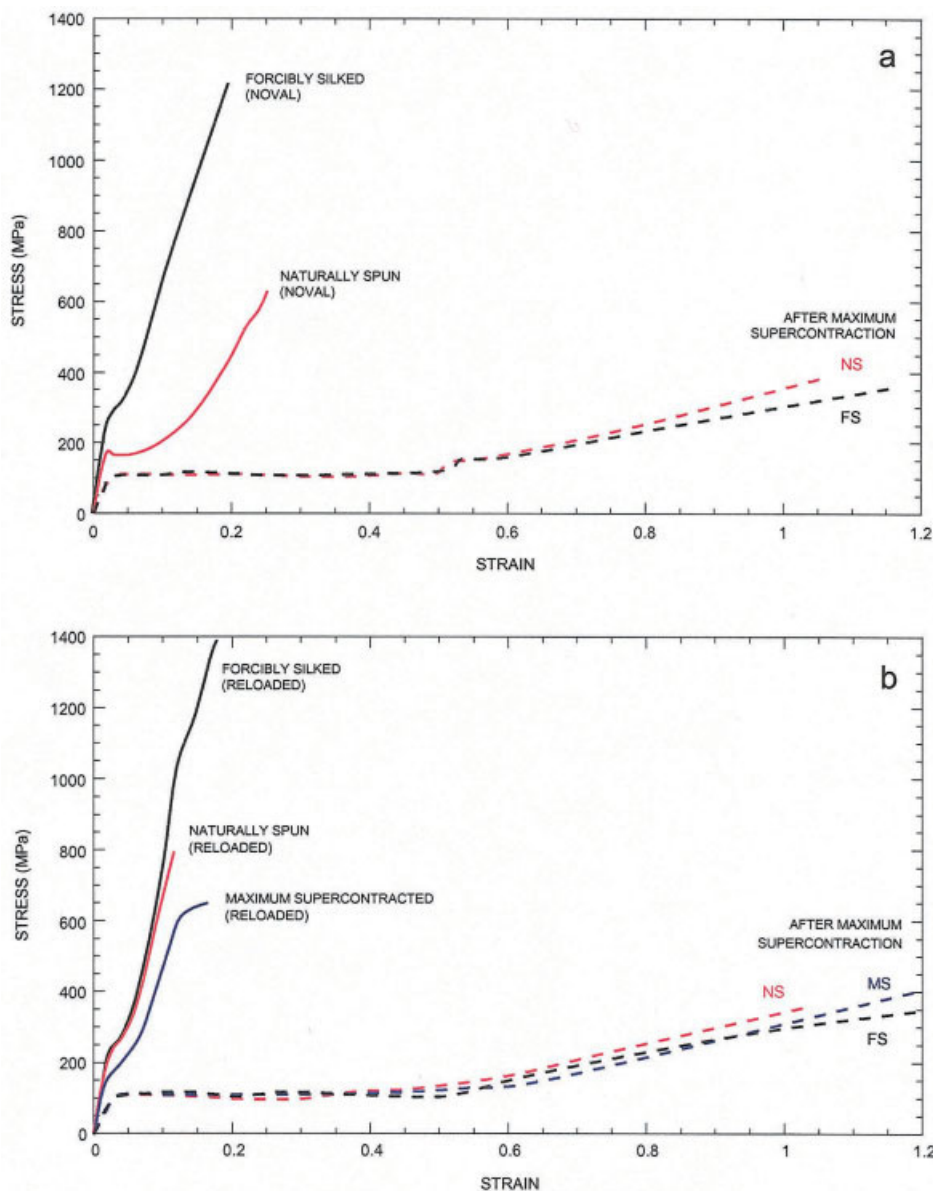


**Figure 2** Stress–strain curves of (a) noval fibers (FS and NS) before and after maximum SC {percentage SC  $[(L_0 - L_C)/L_0] = 57\%$  for FS fibers and  $35\%$  for NS fibers} and (b) reloaded fibers (FS, NS, and MS) before and after recovery due to maximum SC {percentage SC  $[(L_0 - L_C)/L_0] = 58\%$  for FS fibers,  $49\%$  for NS fibers, and  $48\%$  for MS fibers}. Note that all of the final curves coincide after maximum SC.

were recovered through controlled SC. The five curves of the controlled supercontracted fibers were coincident, giving strong support to the reproducibility of the proposed procedure. This reproducibility was checked by at least four tests for each percentage of SC. All of the curves showed differences below 5% in stress at a given strain, except for the scatter in the values of tensile strength.

The possibilities opened up by the recovery ability of spider silk are far-reaching: for the first time, a procedure is available to obtain spider silk fibers with a tailored stress–strain profile, in a reliable and repetitive way, starting from NS, FS, or supercontracted

fibers. Moreover, the process allows the recovery of the tensile properties of fibers after irreversible deformation. This technique should facilitate the planning and interpretation of tensile tests, with subsequent benefits for the biomimetics industry.

A spider drag line can be modeled as a semicrystalline material made of amorphous flexible chains reinforced by polyaniline nanocrystallites. During SC, the nanocrystallites are not disrupted but may rotate from their initial alignment with the axis of the fiber.<sup>20,21</sup> Conformation of the amorphous chains is more controversial because it has been suggested that it could correspond to  $\beta$  sheets,<sup>22</sup>  $3_1$  helix,<sup>23,24</sup> or  $\beta$  turns,<sup>25</sup> but

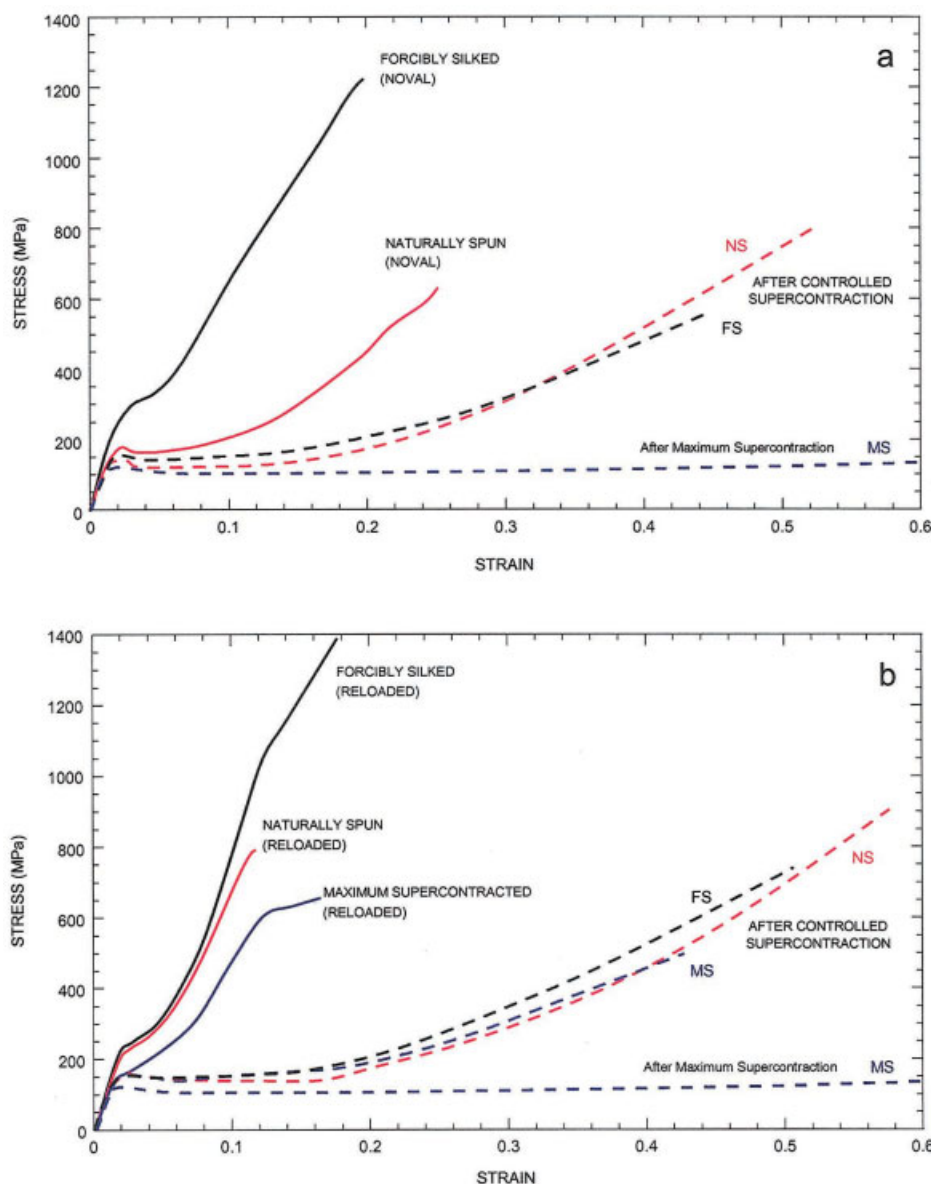


**Figure 3** Stress–strain curves of (a) noval fibers (FS and NS) before and after controlled SC {percentage SC  $[(L_0 - L_C)/L_0] = 25\%$  for FS fibers and  $14\%$  for NS fibers} and (b) reloaded fibers (FS, NS, and MS) before and after recovery due to controlled SC {percentage SC  $[(L_0 - L_C)/L_0] = 16\%$  for FS fibers,  $17\%$  for NS fibers, and  $13\%$  for MS fibers}. Note that the final curve, aimed at reproducing a curve of the NS family,<sup>5</sup> is the same in all five cases. The curve after maximum SC from Figure 2 is included for comparison purposes.

it seems to remain unaffected by SC.<sup>24</sup> In this context, the results presented in this article cast light on the interactions that control the tensile properties of spider silk. The tensile behavior of silk seemed to correspond to an elastomeric material, whose properties were controlled by the alignment of the chains. The independence of the tensile properties from the previous loading history was consistent with this hypothesis. However, the elastomeric behavior only appeared in wet supercontracted fibers since drying freezes the conformation of the chains through an interaction reverted by the presence of water molecules, likely hydrogen bonds.<sup>11,12,17</sup> The amorphous chains

extend during a tensile test in air, dissipating energy, but it has been shown above that these conformational changes are reversible when the humidity is increased and when chain reorientation is allowed. It is likely that this model, together with the controlled SC procedure, could help to explain the mechanical properties of MAS fibers, particularly the stress–strain curves depicted in this article.

## CONCLUSIONS

1. The tensile properties of MS fibers were independent from the previous loading history of the



fiber (noval or reloaded) and from the collection procedure (NS or FS).

2. A judicious combination of controlled SC and stretching allowed us to obtain the whole range of tensile properties exhibited by NS fibers, independently of the loading history of the fiber or the collection technique.
3. The tensile behavior of wet supercontracted fibers was controlled by the reversible alignment of the chains. In this respect, a given conformation could be frozen by a combination of drying and stretching the fiber, a process that it is likely to involve hydrogen bonding between the chains.

*A. trifasciata* specimens were kindly provided by Jesús Miñano. We thank Oscar Campos (Naturaleza Misteriosa, Parque Zoológico de Madrid, Spain) for rearing the spiders and José Miguel Martínez for help with testing samples and drawing figures.

## References

1. Kaplan, D. L.; Lombardi, S. J.; Muller, W. S.; Fossey, S. A. In *Biomaterials: Novel Materials from Biological Sources*; Byrom, D., Ed.; Stockton: New York, 1991; p 1.
2. Lazaris, A.; Arcidiacono, S.; Huang, Y.; Zhou, J.-F.; Duguay, F.; Chretien, N.; Welsh, E. A.; Soares, J. W.; Karatzas, C. N. *Science* 2002, 295, 472.
3. Work, R. W. *Textile Res J* 1976, 46, 485.
4. Griffiths, J. R.; Salinatri, V. R. *J Mater Sci* 1980, 15, 491.
5. Garrido, M. A.; Elices, M.; Viney, C.; Pérez-Rigueiro, J. *Polymer* 2002, 43, 4495.
6. Denny, M. J. *J Exp Biol* 1976, 65, 483.
7. Gosline, J. M.; Guerette, P. A.; Ortlepp, C. S.; Savage, K. N. *J Exp Biol* 1999, 202, 3295.
8. Madsen, B.; Shao, Z. Z.; Vollrath, F. *Int J Biol Macromol* 1999, 24, 301.
9. Work, R. W. *Textile Res J* 1977, 47, 650.
10. Gosline, J. M.; Denny, M. W.; DeMont, M. E. *Nature* 1984, 309, 501.
11. Termonia, Y. *Macromolecules* 1994, 27, 7378.
12. Termonia, Y. In *Structural Biological Materials*; Elices, M., Ed.; Elsevier: Oxford, England, 2000; p 335.
13. Pérez-Rigueiro, J.; Elices, M.; Guinea, G. V. *Polymer* 2003, 44, 3733.
14. Garrido, M. A.; Elices, M.; Viney, C.; Pérez-Rigueiro, J. *Polymer* 2002, 43, 1537.
15. Work, R. W.; Emerson, P. D. *J Arachnol* 1982, 10, 1.
16. Pérez-Rigueiro, J.; Elices, M.; Llorca, J.; Viney, C. *J Appl Polym Sci* 2001, 82, 2245.
17. Pérez-Rigueiro, J.; Viney, C.; Llorca, J.; Elices, M. *Polymer* 2000, 41, 8433.
18. Guinea, G. V.; Elices, M.; Pérez-Rigueiro, J.; Plaza, G. *Polymer* 2003, 44, 5785.
19. Pérez-Rigueiro, J.; Viney, C.; Llorca, J.; Elices, M. *J Appl Polym Sci* 1998, 70, 2439.
20. Work, R. W.; Morosoff, N. *Text Res J* 1982, 52, 349.
21. Grubb, D. T.; Ji, G. *Int J Biol Macromol* 1999, 24, 203.
22. Thiel, B. L.; Kunkel, D. D.; Viney, C. *Biopolymers* 1994, 34, 1089.
23. Kümmerlen, J.; van Beek, J. D.; Vollrath, F.; Meier, B. H. *Macromolecules* 1996, 29, 2920.
24. van de Beek, J. D.; Kümmerlen, J.; Vollrath, F.; Meier, B. H. *Int J Biol Macromol* 1999, 24, 173.
25. Jelinski, L. W.; Blye, A.; Liivak, O.; Michal, C.; LaVerde, G.; Seidel, A.; Shah, N.; Yang, Z. *Int J Biol Macromol* 1999, 24, 197.